

In Vitro Studies of the Antimicrobial and Free-Radical Scavenging Potentials of Silver Nanoparticles Biosynthesized From the Extract of *Desmostachya bipinnata*

Analytical Chemistry Insights
Volume 13: 1–9
© The Author(s) 2018
Reprints and permissions:
sagepub.co.uk/journalsPermissions.nav
DOI: 10.1177/1177390118782877



Sitaramanjaneya Reddy Guntur¹, NS Sampath Kumar²,
Manasa M Hegde³ and Vijaya R Dirisala²

¹Department of Biomedical Engineering, Vignan's Foundation for Science, Technology & Research (Deemed to be University), Guntur, India. ²Department of Biotechnology, Vignan's Foundation for Science, Technology & Research (Deemed to be University), Guntur, India.

³Department of Nanotechnology, Rajiv Gandhi Institute of Technology, Bangalore, India.

ABSTRACT: The aim of this study was to perform green synthesis of silver nanoparticles (AgNPs) from the leaf extract of *Desmostachya bipinnata* (Dharba), a medicinally important herb which is widely used across India. Synthesized AgNPs were analyzed by UV-Visible spectroscopy, X-ray diffraction (XRD), Fourier transform infrared (FTIR) spectroscopy, scanning electron microscopy (SEM), and energy dispersive X-ray spectroscopy (EDAX). The results have confirmed that green synthesis of AgNPs leads to the fabrication of sphere-shaped particles with a diameter of 53 nm. Furthermore, these AgNPs were subjected to antioxidant and antimicrobial studies against gram-negative and gram-positive bacteria, where AgNPs at a concentration of 20 mg/mL showed highest zone of inhibition. Synthesized AgNPs were evaluated for their antioxidant activity by 1, 1-diphenyl-2-picryl hydrazyl radical (DPPH), H₂O₂, and superoxide inhibiting assays; increasing concentration has showed increase in scavenging ability. Cell toxicity was assessed on HepG2 cell lines, and synthesized nanoparticles at a concentration of 128 µg/mL produced significant reduction in viability of Hep cells ($P < .05$). The availability of Dharba throughout the year and the eco-friendly approach in the synthesis of AgNPs coupled with bioactivity has demonstrated its potential as a novel biomaterial which can be used for various biomedical applications.

KEYWORDS: *Desmostachya bipinnata*, silver nanoparticles, antimicrobial activity, antioxidant activity, green synthesis

RECEIVED: December 7, 2017. **ACCEPTED:** May 3, 2018.

TYPE: Research article

FUNDING: The author(s) received no financial support for the research, authorship, and/or publication of this article.

DECLARATION OF CONFLICTING INTERESTS: The author(s) declared no potential conflicts of interest with respect to the research, authorship, and/or publication of this article.

CORRESPONDING AUTHOR: Vijaya R Dirisala, Department of Biotechnology, Vignan's Foundation for Science, Technology & Research (Deemed to be University), Vadlamudi, Guntur 522213, Andhra Pradesh, India. Email: drdirisala@gmail.com

Introduction

Research on nanoparticles is inevitable today because of their applicability in various fields as they possess catalytic, optical, magnetic, biological, and distinct physiochemical properties.^{1,2} These properties are strongly influenced by degree of temperature, polarity of solvent, concentration of precursors, and reduction agents.³ On a special note, silver nanoparticles (AgNPs) display remarkable applications in the field of medicine for therapeutics and diagnostics as they are eco-friendly.⁴ Moreover, biological activities of AgNPs results in enhanced treatment quality, reduced side effects, and improved quality of life which in turn significantly influences the overall performance of the system.⁵ Silver nanoparticles can be fabricated by different methods, which include physical, chemical, and biological.^{6–8} Even though physical and chemical methods yield high amount of NPs with specific size and shape, usage of microorganisms or enzymes or plant extracts related to biological practices are considered to be environment friendly, reliable, nontoxic, and prudent.^{9,10}

Synthesizing of nanoparticles using plant extracts is considered as green synthesis and various medicinal and aromatic plant extracts of neem (*Azadirachta indica*),¹¹ guava (*Psidium guava*),¹² lemon (*Citrus lemon*),¹³ *Chenopodium murale*,¹⁴ *Pulicaria*

glutinosa,¹⁵ and so on were used by various researchers. Metabolites Viz., polyphenols, flavonoids, terpenoids, and tannins present in the plant extracts act as reducing agents that are beneficial in decreasing the particle size.^{16–18} This process not only influences the morphology and stability of nanoparticles but also enhances their biological properties. Therefore, biological method synthesizing gold nanoparticles and AgNPs by various extracts prepared from plants has gained considerable importance in biomedical applications,^{19–22} and recently AgNPs are widely used as antimicrobial and antioxidant agents.^{23–29}

Desmostachya bipinnata is a medicinally important herb commonly known as dharba, belonging to the Poaceae family. It is considered as holy grass and comprehensively used in Indian Vedic practices during rituals. It is well known for its medicinal value and is used in traditional Indian medicine (Ayurveda) to treat diseases such as bladder infections, jaundice, menorrhagia, hemorrhoids, dysentery, diarrhea, urinary calculi, and dysuria and asthma.^{30–33} Leaf extracts of *D. bipinnata* (Db) were used as antiulcerogenic, analgesic, antipyretic, and anti-inflammatory. Shortage of significant therapeutic agents to treat persistent global diseases identification of new methods/molecules to address these issues is the need of hour.



Creative Commons Non Commercial CC BY-NC: This article is distributed under the terms of the Creative Commons Attribution-NonCommercial 4.0 License (<http://www.creativecommons.org/licenses/by-nc/4.0/>) which permits non-commercial use, reproduction and distribution of the work without

further permission provided the original work is attributed as specified on the SAGE and Open Access pages (<https://us.sagepub.com/en-us/nam/open-access-at-sage>).



Figure 1. Photograph of the *Desmostachya bipinnata* grass leaf.

Based on the literature available in Ayurveda and information passed from various generations as Folk medicine,³⁴ *D. bipinnata* (Db) extracts can be used as alternative medicine for treating various microbial diseases. Considering its therapeutic importance and to add a new dimension, aim of this study is to employ the leaf extract of *D. bipinnata* (Db) for synthesizing the AgNPs. The synthesized AgNPs was characterized by using different techniques, namely, UV-Visible (UV-Vis) spectroscopy, X-ray diffraction (XRD), Fourier transform infrared spectroscopy (FTIR), scanning electron microscopy (SEM), and energy dispersive X-ray spectroscopy (EDAX) analysis. Silver nanoparticles were further used in in vitro analysis of the antimicrobial activity on various bacteria and fungi, such as *Escherichia coli* (urinary tract toxicities), *Staphylococcus aureus* (skin and blood stream epidemics), *S. mutans* (oral cariogenic decays), and *Candida albicans* (oropharyngeal candidiasis), and analyzed for their antioxidant potential. Furthermore, they were also assessed for their effect on in vitro cell viability assay which can be used for future biomedical applications.

Materials and Methods

D. bipinnata (Db) leaf extract

D. bipinnata (Db) leaves as shown in Figure 1, were collected from the Western Ghats, Karnataka, India. Leaves were cleaned thoroughly under running water and double-distilled water to get rid of the extraneous materials. Sample was chopped and desiccated at 60°C for about 7 days and powdered using a grinder. About 10 g of the powdered sample was placed in a flask containing 100 mL of distilled water and boiled at 60°C in water-bath for 15 minutes and subsequently brought to room temperature. The extract was filtered using a Whatman No 1 filter paper (Z274852, Grade 1, Sigma-Aldrich, Merck, USA) and subsequently used to synthesize AgNPs.

Preparation of silver nanoparticles

A total of 1.5 g of high-analytical grade silver nitrate (0.1 M AgNO₃, ACS reagent, ≥ 99.0%, Sigma-Aldrich, Merck, USA)

was dissolved in 90 mL of High performance liquid chromatography (HPLC) grade water to form AgNO₃ solution. Approximately 15 mL of the *D. bipinnata* (Db) extract was mixed with the AgNO₃ solution in a ratio of 1:3 and placed on a magnetic stirrer for 15 minutes. The resulting solution was kept in the dark for 24 hours to observe the changes in color, which represents the reduction of silver.

Characterization of the silver nanoparticles

Synthesized AgNPs were analyzed by using dispersive methods, such as UV-Vis spectrophotometer (Perkin-Elmer, Lambda 35, USA), FTIR Spectrometer (Perkin Elmer Spectrum 2, wavelength range of 8000–350 cm⁻¹, USA), X-ray diffractor (EDX, Siemens, Model D8, Aubrey, Texas, USA), Scanning electron microscope (SEM; TESCAN/VEGA, Model 3, USA), and EDX (Siemens, Model D8, Aubrey, Texas, USA). Fourier transform infrared spectrometer is useful in characterizing functional groups, bonding types, and nature of the compounds. The AgNP solution was centrifuged at 15 000 r/min to obtain AgNPs in powdered form and loaded in a sample holder and detected in the range of 4000 to 400 cm⁻¹ using the KBr method. The scanning electron microscope was used to observe the morphology and composition of the AgNPs coupled with EDX to identify the elemental composition of the materials. Data generated by the EDX analysis consisted of the spectra of various peaks. The TEAM EDS point analysis software was used for the EDAX analysis to identify the element present in the sample. The phase variations and trace dimension of AgNPs were determined using X-ray diffractometer with Cu Kα radiation and Ni filter. The following Scherer's equation was used to calculate the size of the prepared samples.

$$D = \frac{0.9\lambda}{\beta \cos\theta} \quad (1)$$

where, D is the crystal size, λ is the wavelength of X-ray, θ is the Bragg's angle in radians, and β is the full width at half maximum of the intensity peak in radians. The ultrafine AgNPs powder was characterized at 2θ of 5° to 80°.

In vitro antimicrobial properties of the silver nanoparticles

In vitro antimicrobial activity was investigated using the test samples (Db extracts/AgNPs) dispersed in 1 mL of sterilized distilled water and autoclaved (7440PAD, Medical Instruments, Mumbai, India) for 30 minutes. The bacterial strain cultures of *E. coli* (MCC 2079), *S. aureus* (7443, MTCC), *S. mutans* (1943, MTCC), and *C. albicans* (MCC 1154) were used to investigate the antimicrobial activity by utilizing the well-plate method using Mueller-Hinton agar (M173, Hi Media Laboratories, Mumbai, India). The culture media were prepared by dissolving 13 g of nutrient broth (M001, Hi Media Laboratories,

Mumbai, India) powder in 1000 mL of distilled water. The sample medium for the antifungal activity was prepared using 250 g of peeled potato in a beaker with 800 mL of distilled water, boiled for 20 minutes on a hot plate. The boiled potato was squeezed and filtered using a Whatman filter paper. A total of 20 g of dextrose (GRM-007, HiMedia Laboratories, Mumbai, India) was added to the filtrate, and the volume was adjusted by adding 1000 mL of distilled water and used for analysis. Ampicillin and fluconazole (HiMedia Laboratories, Mumbai, India) were used as the standard drugs against bacteria and fungi, respectively. The Db extracts and AgNPs were separated according to their antimicrobial actions by the Kirby-Bauer disc diffusion method to determine the zone of inhibition.³⁵ Measurements with different concentrations of the grass leaf extracts and AgNPs (10, 15, and 20 mg/mL) and standard antibiotics were repeated for the test organisms and recorded for their zone of inhibition (mm).

Radical scavenging ability of silver nanoparticles

DPPH radical scavenging assay. Reducing ability of Db extract and AgNPs were assessed using the 1, 1-diphenyl-2-picrylhydrazyl radical (DPPH) assay method. For each concentration (1, 10, 15, and 25 µg/mL), 1 mL of the sample was added with 3 mL of DPPH solution (0.004%). The prepared solution was left for 15 to 20 minutes in a dark room and read at 517 nm by UV-Vis spectrophotometer (PerkinElmer, Lambda 35, Germany). The percentage of inhibition was calculated using the formula

$$\text{Inhibition of DPPH radicals (\%)} = \left[\frac{A_c - A_t}{A_t} \right] \times 100, \quad (2)$$

where A_c is absorbance of control sample (DPPH solution without test sample), and A_t is the absorbance of test sample (DPPH solution with test sample).

Reactive oxygen species (H_2O_2) scavenging assay. Reactive oxygen species (H_2O_2) was mixed in buffer with a known concentration and pH (30 mM; 7.4). Measures of 1.5 mL of samples (NPs) in different ratios or standards (α -Tocopherol and Ascorbic acid) were added to 2.5 mL of H_2O_2 and read at 233 nm after incubation.

Superoxide radical scavenging assay. Various concentrations of 0.5 mL AgNPs were diluted in 1 mL of basic Dimethyl sulphoxide (DMSO: 6 mM NaOH), and 0.1 mL of nitroblue tetrazolium in 2.5 mg/mL concentration was added to make a final mixture and read at 565 nm.

In vitro cell viability assay

The HepG2 (human liver cancer cell line) were grown and maintained in DMEM (Dulbecco Modified Eagle Medium) which was supplement with 10% Fetal bovine serum (FBS),

2 mM L-glutamine 100 U/mL penicillin G sodium and 100 mg/mL streptomycin sulphate. Cells were seeded in 96-well plate at a density of 1×10^4 cells/mL along with aforementioned media and maintained at 37°C and humidified with 5% CO_2 . HepG2 cells after reaching confluence were tested with various concentrations of synthesized AgNPs for cytotoxicity. After 24 hours of incubation, medium was discarded and the adherent cells were washed thrice with PBS and 30 µL of 3-(4,5-dimethyl-2-thiazolyl)-2,5-diphenyl-tetrazolium bromide (MTT; 10 mg/mL in PBS) was added to each well and incubated for 6 hours. Then 70 µL of DMSO was added to each well to solubilize the formazan crystals produced by viable cells. Furthermore, the absorbance was measured at 540 nm, as reference wavelength using a multiscan spectrophotometer (microplate reader) (Waltham, MA, USA). The effect of the AgNPs on the proliferation of HepG2 cells was expressed as the percent of cell viability using the following formula:

$$\% \text{ Proliferation} = \left[\frac{OD_{\text{sample}} - OD_{\text{control}}}{OD_{\text{control}}} \right] \times 100.$$

Results and Discussion

Preparation and optimization of nanoparticles

The Db extract was mixed to silver nitrate solution and incubated for 24 hours, thereby resulting in the change in the intensity color from light brown to dark due to reduction of Ag^+ to Ag^0 . This attributes to the phenomenon of surface plasmon resonance (SPR) absorption band which is found in noble metals as a result of vibrations that are in tune with the light wave of both electrons in metal NPs. The maximum degradation of the Ag^+ ions was observed after 4 hours of adding the grass leaf extract to the $AgNO_3$ solution. The absorbance was measured from 300 to 700 nm using UV-Vis spectrophotometer which showed SPR hike at 433 nm confirming the formation of AgNPs as shown in Figure 2A. Mie theory suggested that the absorption spectra of a single spherical NP SPR band are possible; in addition, the peak increases with increased anisotropy.³⁶ The parameters measured in the AgNPs extract of *D. bipinnata* (Db) leaf are similar to those of previous measurements that used other plants, namely, *Terminalia chebula*, *Ocimum sanctum*, *Syzygium cumini*, *Piper nigrum*, and *Foeniculum vulgare* resulted in the maximum absorbances at 452, 452, 427, 420, and 475 nm, respectively.^{35,37,38} Distinct change in color was observed between 3 different concentrations ranging from yellowish to reddish brown for 0.5 to 1.5 mM of silver nitrate. The SPR of synthesized AgNPs became evident with increase in the percentage of silver nitrate and 1.5 mM of $AgNO_3$ (Figure 2B) showed highest peak. Similar effect was noted for change in temperature, when reaction mixtures were incubated at 30°C, 60°C, and 90°C. Increase in the temperature has increased the SPR peak as shown in Figure 2C; moreover, it has also reduced the time taken for formation of AgNPs. Previous studies have also confirmed

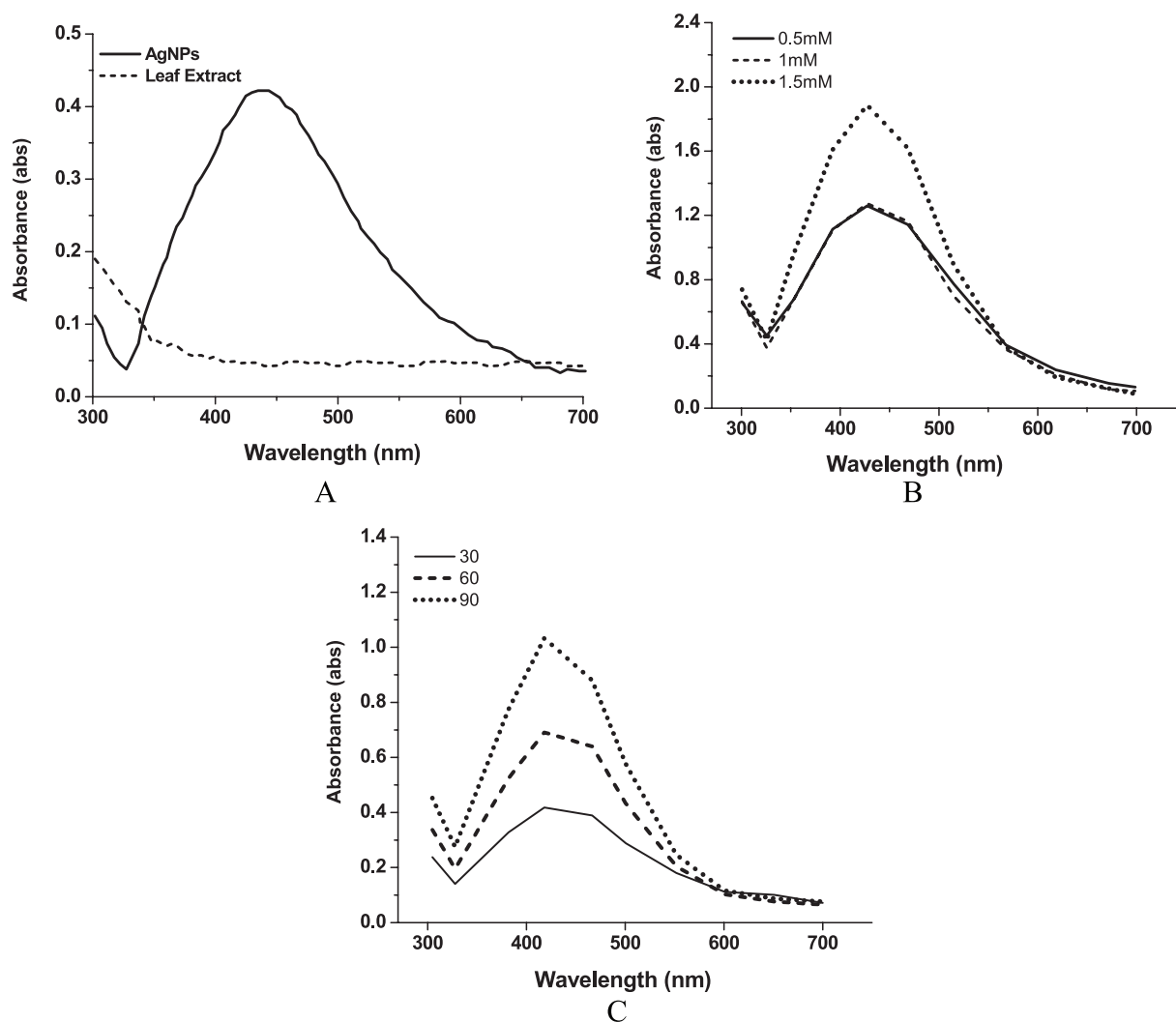


Figure 2. (A) Typical UV-Vis absorption spectra of the *D. bipinnata* (Db) leaf extract with the AgNPs. *D. bipinnata* (Db) leaf extract is showing the absorption peaks at 348 nm and the AgNPs show the SPR peak at 433 nm. (B) The SPR peak of AgNPs with concentration of AgNO₃ at 0.5, 1, and 1.5 mM. (C) The SPR peak of AgNPs incubated at temperatures 30°C, 60°C, and 90°C. AgNP indicates silver nanoparticle; SPR, surface plasmon resonance; UV-Vis, UV-Visible.

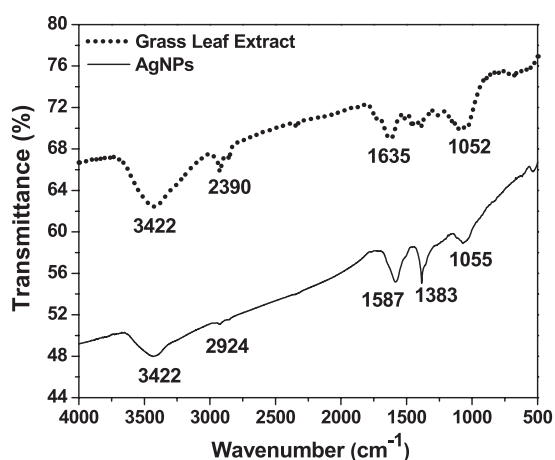


Figure 3. Typical Fourier transform infrared spectrum of the *D. bipinnata* (Db) leaf extract with the AgNPs shows the presence of a range of functional groups. The *D. bipinnata* (Db) leaf extract contains alcohols, carboxylic acids, esters, and ethers. The AgNPs contain flavonoids, terpenoids, phenols, and aromatic compounds. AgNP indicates silver nanoparticle.

similar change in the shift of SPR band based on the level of nanoparticles fabrication and sometimes because of the secondary metabolites responsible for the synthesis.^{25–29}

Physicochemical characterization of nanoparticles

Fourier transform infrared spectrum (Figure 3) for the Db extract and NPs was performed to examine the stabilization of nanoparticles through biomolecules as capping agents. Grass leaf extract showed several spectral peaks such as, 3422 cm⁻¹, which corresponds to the oxygen-hydrogen stretch to the Hydrogen-bonded OH groups and phenols which indicates complex nature of biomolecules. The peak obtained at 2390 cm⁻¹ confirms O–H and C–H stretching bonds, which corresponds to carboxylic acids, primary amines, and alkanes.³⁰ The findings are further supported by a peak at 1635 cm⁻¹ representing amines through H–N bond. Another peak (1052 cm⁻¹) represents the C–O and C–H stretching bonds, which indicated the availability of functional groups.³⁶

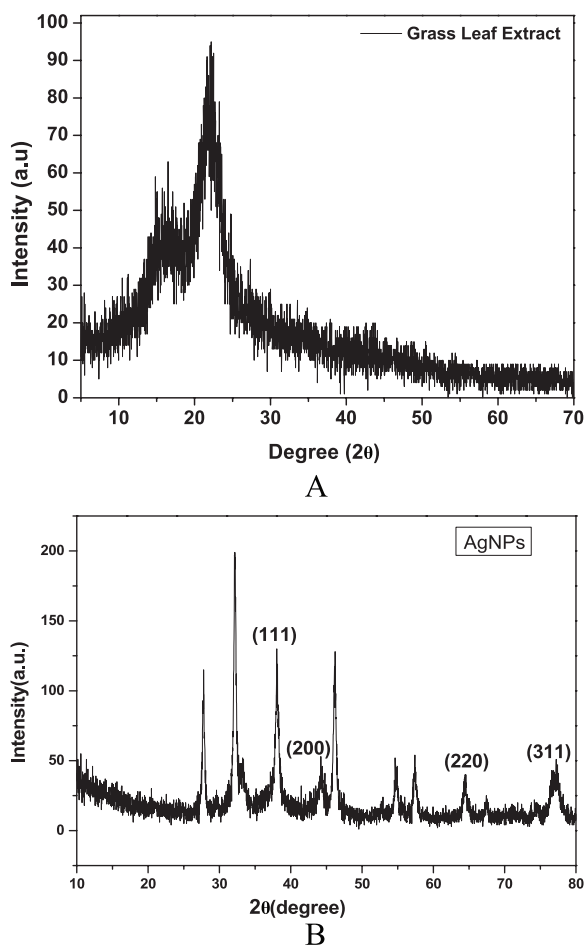


Figure 4. X-ray diffraction spectra: (A) *D. bipinnata* (Db) leaf extract shows the peak at 21.9°, which corresponds to the diffraction plane (011). (B) AgNPs show the peaks at 38.1°, 44.3°, 64.4°, and 77.4°, which correspond to the diffraction planes (111), (200), (220), and (311), respectively. AgNP indicates silver nanoparticle.

The FTIR spectrum of the AgNPs with respect to the percentage of transmittance as the function of wavelength showed a few similar peaks corresponding to the presence of phenolic and alkanes interaction.²⁷ Other peaks at 1587 cm^{-1} and 1383 cm^{-1} corresponding to the C–C stretching bond indicates the presence of aromatic compounds and the N–O symmetric stretching that demonstrated the presence of the nitro compounds, respectively.²⁸ The peak at 1055 cm^{-1} represented the C–O and C–H stretching bonds, which corresponded to the presence of alcohols, carboxylic acids, esters, ether, and aliphatic amines.³⁹ Consequently, the synthesized AgNPs were bound by various proteins and metabolite functional groups containing terpenoids/flavonoids must have improved the ability to form a capping agent.²⁹

The Db extract showed the maximum peaks at 21.99° on XRD spectrum, which corresponded to the 011 diffraction planes indicating the microcrystalline nature of the *D. bipinnata* (Db) confirming high carbon and oxygen contents. In contrast to the leaf extract, AgNPs showed prominent crest of 2θ starting from 38.1°, 44.3°, 64.4°, and 77.4°, which are related to the diffraction planes (111), (200), (220), and (311),

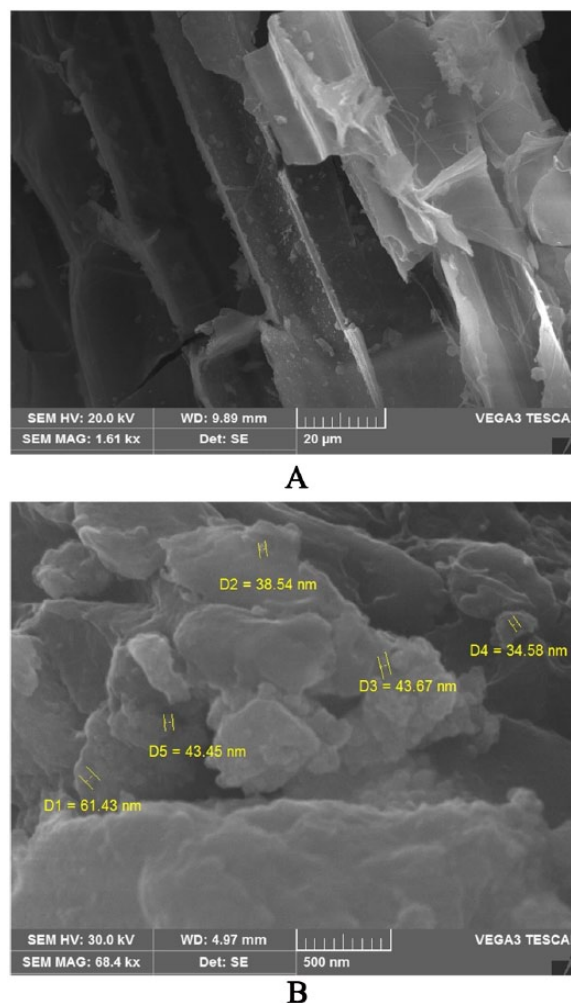


Figure 5. Scanning electron microscopy (SEM) images: (A) *D. bipinnata* (Db) leaf extract is represented by a hexagonal shape. (B) AgNPs are represented by a spherical shape with a diameter ranging from 30 to 60 nm. AgNP indicates silver nanoparticle.

respectively (Figure 4B). These diffractions are related to the face-centered cubic configuration of AgNPs with average diameters of 132 μm and 53.3 nm estimated using Debye Scherer equation (1). The sharp peak at 38.1° was due to the stabilization of nanoparticles caused by the capping agent, which may be further responsible for powerful X-ray scattering layers as proposed in Strong Bragg reflections. Hence, the XRD spectrum showed that AgNPs were crystalline in nature and expected to be small in particle size; these results were in agreement with previous investigations.^{39–41}

The SEM analysis verified the surface morphology and dimensions of the samples (Figure 5). The grass leaf extract showed hexagonal shape and AgNPs exhibited regular round-shaped particles within the range of 30 to 60 nm in diameter (Figure 5B). These superficial impurities may be due to the presence of biocapping agents of the unrefined fractions from the Db extract.³⁷ X-ray diffractor spectral analysis (Figure 6A and B) detected the presence of elements within the selected area and found 78.27% of Ag as the major element in the sample with carbon (18.06%) and oxygen (3.67%) as other

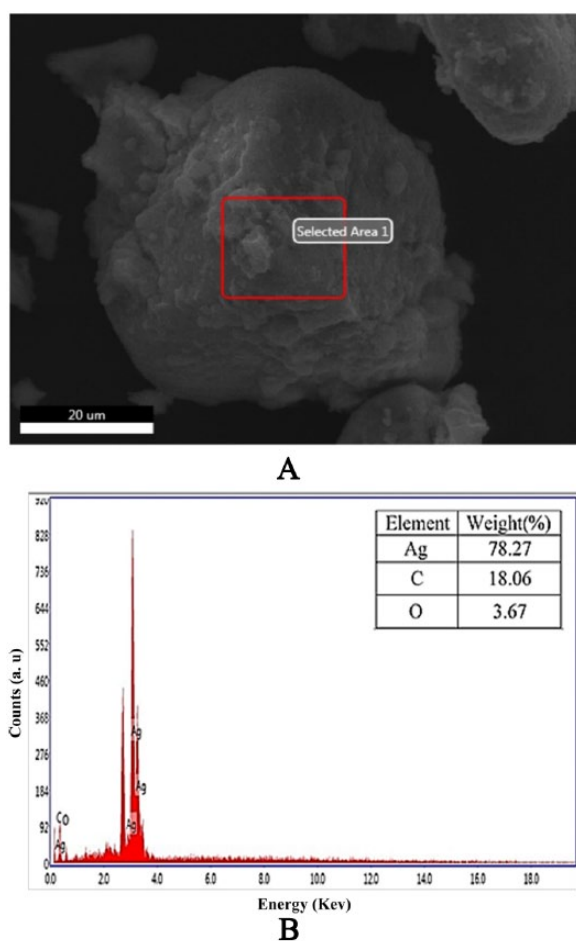


Figure 6. EDX spectrum: (A) Rectangular area of the AgNPs from the SEM image was selected for analysis. (B) EDX spectrum was measured from the selected area of (A). AgNP indicates silver nanoparticle; EDX, X-ray diffractor; SEM, scanning electron microscopy.

elements. The significant amount of carbon and small amount of oxygen in the sample indicated the various physiochemical properties of AgNPs in the form of biocapping agent. The SEM and EDAX analyses showed no clear morphology of the formed AgNPs.^{42–44}

Antimicrobial properties of the silver nanoparticles

Green synthesized AgNPs were planned to use as a substitute for conventional antibiotics to fight against intracellular pathogenic bacteria, especially for the drug-resistant bacteria.³⁹ Figure 7 illustrates the antimicrobial activity against *E. coli*, *S. aureus*, *S. mutans*, and *C. albicans* with the zone of inhibition at different concentrations (10, 15, and 20 mg/mL) for synthesized AgNPs. The antimicrobial actions of the AgNPs decreased with the decrease in concentration of the test sample as shown in Table 1 in comparison with standard drug. Silver nanoparticles at a concentration of 20 mg/mL showed highest inhibitory zone for *E. coli*, *S. aureus*, and *S. mutans* with a diameter of 13.5 ± 1 , 21 ± 1 , and 18.5 ± 1.3 mm which was very close to the standard ampicillin with 100 mg/mL concentration

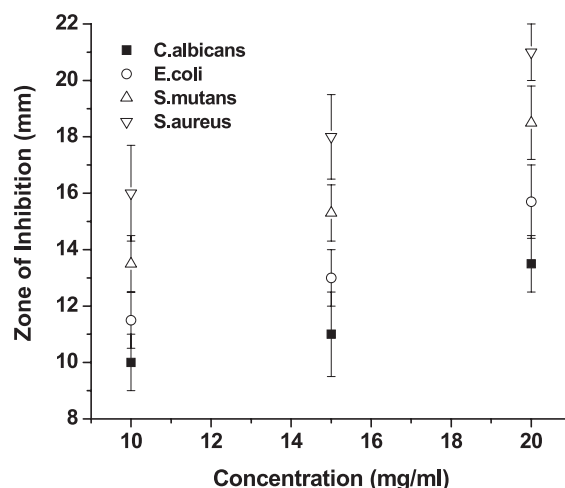


Figure 7. Antimicrobial activity of *Escherichia coli*, *Staphylococcus aureus*, *Staphylococcus mutans*, and *Candida albicans* against the inhibition zone of standard drug (100 mg/mL) and various AgNP concentrations (10, 15, and 20 mg/mL). Data point and error bar represent the mean and standard deviation, respectively, which were obtained in 3 repeated measurements on different samples. AgNP indicates silver nanoparticle.

(Figure 7). The inhibition was remarkably distinct for *S. aureus* as a gram positive bacterium. Even though lot of literature was available on various strategies exhibited by AgNPs for antimicrobial properties, their actual mechanisms are not fully understood.²² Based on the obtained result, bacteria with peptidoglycan membrane were less resistant to the AgNPs when compared with bacteria without that membrane. This variation in interface of AgNPs could be due to the divergence in basic structural design of cell walls between the bacterial groups.³⁰ Many results on antimicrobial activities with various medicinal plants reported that the zone of inhibition of AgNPs ranges from 8 to 11 mm.^{42–45}

Radical scavenging ability of silver nanoparticles

Neutralizing free radicals and other oxidants causes harmful effects to the human body because it consists of complex system of natural enzymatic and non-enzymatic antioxidant resistances.^{23–25} The free radicals are responsible for initiating various diseases like Parkinson disease, neural disorder, mild cognitive impairment, and aging.^{21,27} These free radicals can be protected by the intake of necessary dietary antioxidants.²⁹ The antioxidant intake improves the quality of life by preventing the occurrence of various degenerative diseases cost-effectively.²² Antioxidant properties of Db extract and synthesized AgNPs was assessed against various free radicals such as DPPH, Hydrogen peroxide, superoxide and compared the same with standards, α -Tocopherol, and Ascorbic acid (Figure 8A to C). All the assays confirmed significant antioxidant activity of green synthesized AgNPs which indicates the direct role of secondary metabolites, namely, phenolic compounds, terpenoids, and so on in removing exposed radicals. DPPH

Table 1. Measured antimicrobial activity of *Escherichia coli*, *Staphylococcus aureus*, *S. mutans*, and *Candida albicans* with the inhibition zones (in mm) of the AgNPs and the standard drug (ampicillin). Measurements were repeated 3 times on different samples to obtain their means and standard deviations.

SAMPLE	ZONE OF INHIBITION (MM)			
	AGNPS			STANDARD DRUG (AMPICILLIN)
	10 MG	15 MG	20 MG	
<i>E. coli</i>	10 ± 1.1	11 ± 1.5	13.5 ± 1	18
<i>S. aureus</i>	16.0 ± 1.7	18.0 ± 1.5	21.0 ± 1.0	25
<i>S. mutans</i>	13.5 ± 1	15.3 ± 1.1	18.5 ± 1.3	20
<i>C. albicans</i>	10 ± 1.1	11.0 ± 1.5	13.0 ± 1	18

Abbreviation: AgNP, silver nanoparticle.

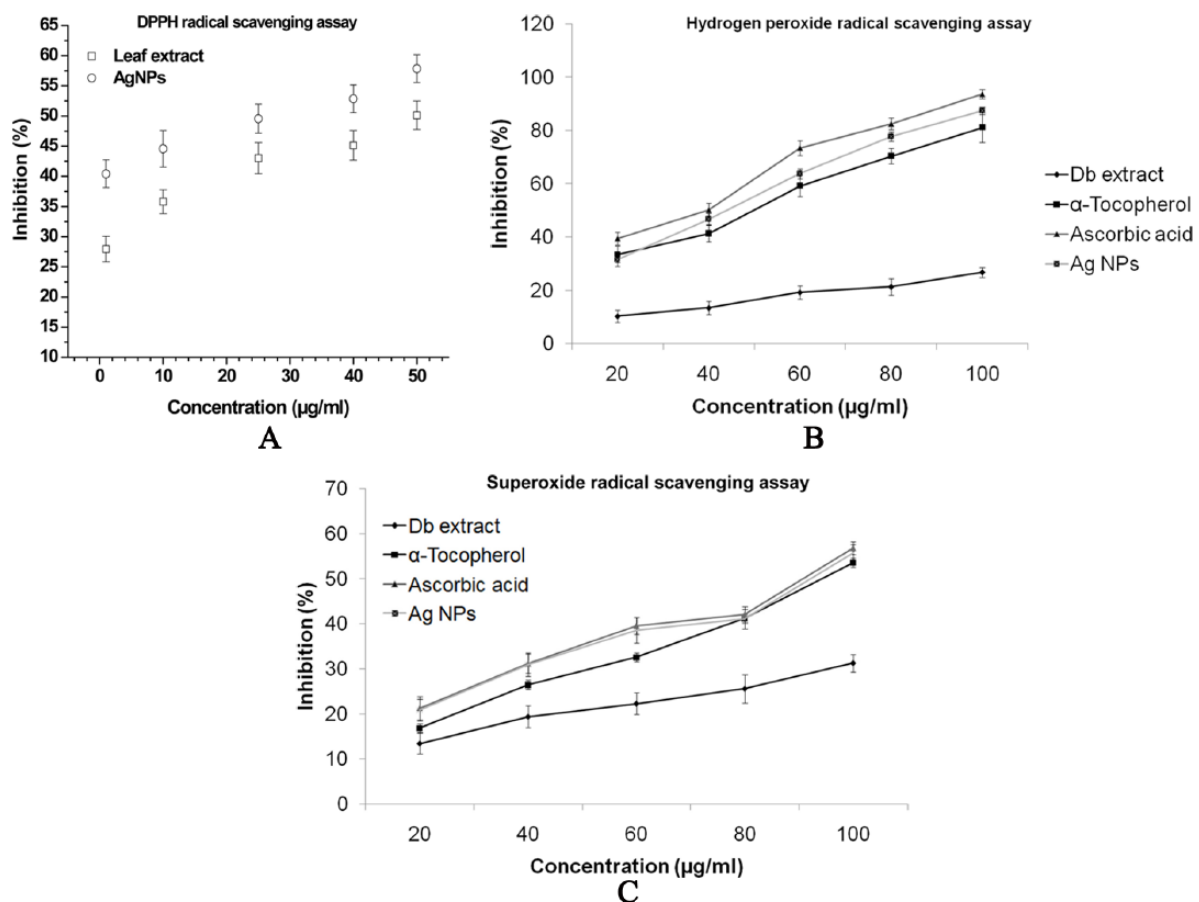


Figure 8. Antioxidant activity of the *D. bipinnata* (Db) leaf extract and the AgNPs at different concentrations demonstrated the percentage of inhibition: (A) DPPH radical scavenging assay. (B) Hydrogen peroxide radical scavenging assay. (C) Superoxide radical scavenging assay. Data point and error bar represent the mean and standard deviation, respectively, which were obtained in 3 repeated measurements on different samples. AgNP indicates silver nanoparticle; DPPH, 1, 1-diphenyl-2-picryl hydrazyl radical.

radical solution which showed a deep purple color with maximum absorbance at 517 nm turns into yellow color when it accepts electron. Discoloration of DPPH started after adding AgNPs due to the antioxidant ability; radical scavenging activity of the Db extract increased with concentration from 1 to 50 µg/mL in the percentage of inhibition ranging from 27.9% ± 2.1% to 50.12% ± 2.37% (Figure 8A). The AgNPs

exhibited the highest percentage of inhibition of 44.41% ± 2.3% even with the lowest concentration of 1 µg/mL. Nevertheless, the lowest concentration of the AgNPs (1 µg/mL) exhibited the highest percentage of inhibition, which is similar to that of the 50 µg/mL Db extract. Hydrogen peroxide is the most commonly generated reactive oxygen species inside the cell and leads to the formation of in vivo hydroxyl radical (OH^{*}). In this

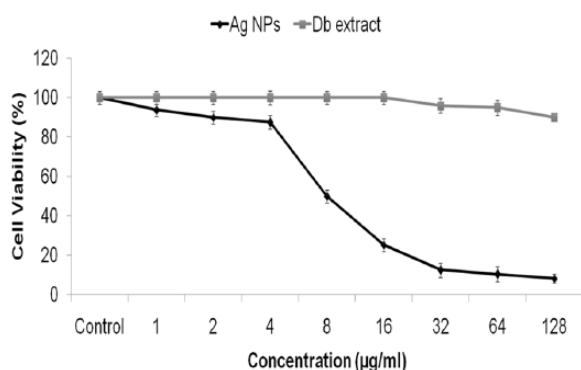


Figure 9. In vitro cell proliferation assay of Hep cells treated with AgNPs and *D. bipinnata* (Db) extract. Values are expressed as mean \pm SD of 3 experiments. AgNP indicates silver nanoparticle.

method, test samples decayed hydrogen peroxide on incubation and the same was spectrophotometrically measured at 230 nm (Figure 8B). The order of the antioxidant activity improved with increase in the concentration but varied between the samples (ascorbic acid > AgNPs > α -Tocopherol > Db extract). Generation of superoxide radical through addition of NaOH to DMSO is another standard and highly accepted method to assess the inhibition of reactive oxygen species. Silver nanoparticles showed better superoxide scavenger capability than α -Tocopherol and very close to the activity of ascorbic acid in inhibiting the formation of a red dye formazan as shown in Figure 8C. Nanoparticles showed excellent antioxidant activity compared with that of the Db extract or other medicinal plants.^{46,47}

In vitro cell viability assay

Toxic effects of AgNPs at 0, 1, 2, 4, 8, 16, 32, 64, and 128 μ g/mL concentration for HepG2 cells was determined using MTT assay. Results have confirmed that nanoparticles up to the concentration of 128 μ g/mL observed a significant decrease in viability of HepG2 cells ($P < .05$). The reduction in viability of AgNPs occurred in a concentration dependent manner as shown (Figure 9). HepG2 cell death increased by $50.1\% \pm 4.1\%$ to $3.3\% \pm 4.5\%$, at 8 to 128 μ g/mL doses, respectively. As the graph clearly shows in Figure 9, the extract of *D. bipinnata* (Db) has not caused any cell death; hence, the effect is solely caused by the AgNPs.

Conclusions

This work describes synthesizing of silver nanoparticles by exposing them to *D. bipinnata* (Db) extract in an eco-friendly process without using any external precursor. Physico-chemical characterization has confirmed the fabricated AgNPs with an average particle diameter of 53 nm with 78% Ag content. These AgNPs showed efficient antimicrobial, antioxidant, and anti-proliferative activity which had demonstrated great potential and definitely will act a significant role in medical device fabrication in the future.

Acknowledgements

Authors would like to thank the management, Vignan's Foundation for Science, Technology & Research, India, for providing administrative and research support.

Author Contributions

SRG conceived the idea and designed the methodology. SRG, VRD, NSSK, MMH performed the assays. VRD and SRG analyzed and interpreted the results. VRD gave critical comments. SRG and VRD prepared the final draft.

REFERENCES

- Ocsoy I, Tasdemir D, Mazicioglu S, Celik C, Katı A, Ulgen F. Biomolecules incorporated metallic nanoparticles synthesis and their biomedical applications. *Mater Lett.* 2018;212:45–50.
- Karatoprak GŞ, Aydin G, Altinsoy B, Altinkaynak C, Koşar M, Ocsoy I. The effect of Pelargonium endlicherianum Fenzl. root extracts on formation of nanoparticles and their antimicrobial activities. *Enzyme Microb Tech.* 2017;97:21–26.
- Ocsoy I, Gulbakan B, Chen T, et al. DNA-guided metal-nanoparticle formation on graphene oxide surface. *Adv Mater.* 2013;25:2319–2325.
- Chen W, Cai W, Zang L, Wang G. Sonochemical processes and formation of gold nanoparticles within pores of Mesoporous silica. *J Colloid Interface Sci.* 2001;238:291–295.
- Frattini A, Pellegrini N, Nicastro D, de Sanctis O. Effect of amine groups in the synthesis of Ag nanoparticles using aminosilanes. *Mater Chem Phys.* 2005;94:148–152.
- Sengupta S, Eavarone D, Capila I, Zhao GL, Watson N, Kiziltepe T. Temporal targeting of tumour cells and neovasculature with a nanoscale delivery system. *Nature.* 2005;436:568–572.
- Ocsoy I, Paret ML, Ocsoy MA, et al. Nanotechnology in plant disease management: DNA-directed silver nanoparticles on graphene oxide as an antibacterial against *Xanthomonas perforans*. *ACS Nano.* 2013;7:8972–8980.
- Prakash P, Gnanaprakasam P, Emmanuel R, Arokiyaraj S, Saravanan M. Green synthesis of silver nanoparticles from leaf extract of *Mimusops elengi*, Linn. for enhanced antibacterial activity against multi drug resistant clinical isolates. *Colloids Surf B Biointerfaces.* 2013;108:255–259.
- Makarov VV, LovMakarov VV, Love AJ, et al. Green nanotechnologies: synthesis of metal nanoparticles using plants. *Acta Naturae.* 2014;6:35–44.
- Huang J, Li Q, Sun D, et al. Biosynthesis of silver and gold nanoparticles by novel sundried *Cinnamomum camphora* leaf. *J Nanotech.* 2007;18:104–115.
- Daizy P. Green synthesis of gold and silver nanoparticles using *Hibiscus rosa sinensis*. *Physica E.* 2010;42:1417–1424.
- Shankar SS, Rai A, Ahamad A, Sastry M. Rapid synthesis of Au, Ag and bimetallic Au core-Ag shell nanoparticles using neem (*Azadirachta indica*) leaf broth. *J Colloid Interface Sci.* 2004;275:496–502.
- Raghuandan D, Mahesh BD, Basavaraja S, Balaji SD, Manjunath SY, Venkataraman A. Microwave-assisted rapid extracellular synthesis of stable bio-functionalized silver nanoparticles from guava (*Psidium guajava*) leaf extract. *J Nanopart Res.* 2011;13:2021–2028.
- Prathna TC, Chandrasekaran N, Raichur AM, Mukherjee A. Biomimetic synthesis of silver nanoparticles by Citrus limon (lemon) aqueous extract and theoretical prediction of particle size. *Colloids Surf B Biointerfaces.* 2011;82:152–159.
- Khan M, Khan M, Adil SF, et al. Green synthesis of silver nanoparticles mediated by *Pulicaria glutinosa* extract. *Int J Nanomed.* 2013;8:1507–1516.
- Akl MA, Nida MS. Green synthesis of silver nanoparticles by mulberry leaves extract. *Nanosci Nanotech.* 2012;2:125–128.
- Ocsoy I, Demirbas A, McLamore ES, Altinsoy B, Ildiz N, Baldemir A. Green synthesis with incorporated hydrothermal approaches for silver nanoparticles formation and enhanced antimicrobial activity against bacterial and fungal pathogens. *J Mol Liq.* 2017;238:263–269.
- Jorge L, Gardea T, Eduardo Gz Jose RP, Jason GP, Horacio T, Miguel J. Alfalfa sprouts: a natural source for the synthesis of silver nanoparticle. *Langmuir.* 2003;19:1357–1361.
- Susan WP, Carla H, Werner I. Nanosilver—a review of available data and knowledge gap in human and environmental risk assessment. *Nanotoxicology.* 2009;3:109–138.
- Prasad MP, Shekhar S, Rindhe G. Antibacterial activity of seaweed (*Gracilaria*) extracts against human pathogens. *Asian J Biol Life Sci.* 2012;1:219–222.

21. Ingole AR, Khatri NT, Wankhade AV, Burghate DK. Green synthesis of selenium nanoparticles under ambient condition. *Chalcogenide Lett.* 2010;7:485–489.
22. Lalitha A, Subbaiya R, Ponmurugan P. Green synthesis of silver nanoparticles from leaf extract *Azadirachta indica* and to study its anti-bacterial and antioxidant property. *Int J Curr Microbiol Appl Sci.* 2013;2:228–235.
23. Kalaiselvi M, Subbaiya R, Selvam M. Synthesis and characterization of silver nanoparticles from leaf extract of *Parthenium hysterophorus* and its antibacterial and antioxidant activity. *Int J Curr Microbiol Appl Sci.* 2013;2:220–227.
24. Abdel-Aziz MS, Shaheen MS, El-Nekeety AA, Wahhab A. Antioxidant and antibacterial activity of silver nanoparticles biosynthesized using *Chenopodium murale* leaf extract. *J Saudi Chem Soc.* 2014;18:356–363.
25. Asirvatham R, Christina AJM, Murali A. In vitro antioxidant and anticancer activity studies on *Drosera Indica L* (Droseraceae). *Adv Pharm Bull.* 2013;3:115–120.
26. Chandra MS, Sasikala K, Anand T, Vengaiah PC, Krishnaraj S. Green synthesis, antimicrobial and antioxidant effects of silver nanoparticles using *Canthium coromandelicum* leaves extract. *J Microbiol.* 2014;9:142–150.
27. Elumalai EK, Hemachandran PT, Therasa VS, Thirumalai T, David E. Extracellular synthesis of silver nanoparticles using leaves of *euphorbia hirta* and their antibacterial activities. *J Phram Sci.* 2010;2:549–554.
28. Bhumi G, LingaRao M, Savithamma N. Green synthesis of silver nanoparticles from the leaf extract of *Adbtoda vasicanees* and assessment of its antibacterial activity. *Asian J Pharm Clin Res.* 2015;8:62–67.
29. Johnson AS, Obot IB, Ukpong US. Green synthesis of silver nanoparticles using *Artemisia annua* and *Sida acuta* leaves extract and their antimicrobial, antioxidant and corrosion inhibition potentials. *J Mater Environ Sci.* 2014;5:899–906.
30. Pandey A, Sharma SK, Singh L, Singh T. An overview on *Desmostachya bipinnata*. *J Drug Discov Ther.* 2013;7:67–68.
31. Joshi SG. *Medicinal Plants*. New Delhi: Oxford & IBH Publishing Co. Pvt. Ltd.; 2003:318.
32. Amani SA, Nawal HM, Derek JM, Gamal AS. Anti-ulcerogenic activity of extract and some isolated flavonoids from *Desmostachya bipinnata*. *Stapp Res Nat Prod.* 2008;3:76–82.
33. Ibrahim NH, Awaad AS, Alnafisah RA, Alqasoumi SI, El-Meligy RM, Mahmoud AZ. In-vitro activity of *Desmostachya bipinnata* (L.) stapf successive extracts against *Helicobacter pylori* clinical isolates. *Saudi Pharm J.* 2018;26:535–540.
34. Panda S, Choudhury NSK, Patro VJ, Pradhan DK, Jan GK. Analgesic, antipyretic and anti-inflammatory effect of the whole plant extract of *Desmostachya bipinnata* Stapf (Poaceae) in albino rats. *Drug Invent Today.* 2009;1:150–153.
35. Sondi I, Salopek SB. Silver nanoparticles as antimicrobial agent: a case study on *E. coli* as a model for gram-negative bacteria. *J Colloid Interface Sci.* 2004;275:177–182.
36. Amooaghaie R, Saeri MR, Azizi M. Synthesis, characterization and biocompatibility of silver nanoparticles synthesized from *Nigella sativa* leaf extract in comparison with chemical silver nanoparticles. *Ecotoxicol Environ Saf.* 2015;120:400–408.
37. Shahverdi AR, Minaeian S, Shahavedi HR, Jamalifar H, Nohi AA. Rapid synthesis of silver nanoparticles using the culture supernatants of Enterobacteria: a novel biological approach. *Process Biochem.* 2007;42:919–923.
38. Santhosh Kumar T, Rahuman AA, Jayaseelan C, et al. Green synthesis of titanium dioxide nanoparticles using *Psidium guajava* extract and its antibacterial and antioxidant properties. *Asian Pac J Trop Med.* 2014;7:968–976.
39. Stuart B. *Infrared spectroscopy: fundamentals and applications*. Publisher: John Wiley & sons. 2004; ISBN: 978-0-470-85428-0
40. Yallappa S, Manjanna J, Peethambar SK, Rajeshwara AN, Satyanarayana ND. Green synthesis of silver nanoparticles using *Acacia farnasiana* (Sweet acacia) seed extract under microwave irradiation and their biological assessment. *J Clust Sci.* 2013;24:1081–1092.
41. Charusheela R, Chakrabarti T, Sarangi BK, Avatar PR. Synthesis of silver nanoparticles from the aqueous extract of leaves of *Ocimum sanctum* for enhanced antibacterial activity. *J Chem.* 2013;2013:278925.
42. Mohan Kumar K, Sinha M, Shridhara Reddy P. Green synthesis of silver nanoparticles using *Terminalia chebula* extract at room temperature and their antimicrobial studies. *Spectrochim Acta A.* 2012;91:228–233.
43. Prasad R, Swamy VS. Antimicrobial activities of silver nanoparticles synthesized by the bark extract of *Syzygium cumin*. *J Nanopart.* 2013;2013:431218.
44. Showmmyan JJ, Harini K, Pradeepa M, Thyagarajan M, Manikandan R, Venkatachalan P. Rapid green synthesis of silver nanoparticles using seed extract of *Foeniculum vulgare* and screening of its antibacterial activity. *Plant Cell Biotechnol Mol Biol.* 2013;13:31–38.
45. UdayaKumar R, Hazeena Begum V. Antimicrobial studies of some selected medicinal plants. *Anc Sci Life.* 2002;4:230–239.
46. Emmanuel R, Palanisamy S, Chen SM, et al. Antimicrobial efficacy of green synthesized drug blended silver nanoparticles against dental caries and periodontal disease causing microorganisms. *Mater Sci Eng C.* 2015;56:374–379.
47. Duman F, Ocsoy I, Kup FO. Chamomile flower extract-directed CuO nanoparticle formation for its antioxidant and DNA cleavage properties. *Mater Sci Eng C.* 2016;60:333–338.